Journal of Sound and Vibration (1999) **225**(5), 803–829
Article No. jsvi.1999.2271, available online at http://www.idealibrary.com on IDEAL®

A STUDY OF TRANSVERSE NORMAL STRESS EFFECT ON VIBRATION OF MULTILAYERED PLATES AND SHELLS

E. CARRERA

Department of Aeronautics and Aerospace Engineering, Politecnico di Torino, Corso Duca degli Abruzzi, 24, 10129 Torino, Italy

(*Received* 10 *September* 1998, *and in final form* 27 *January* 1999)

This paper evaluates transverse normal stress σ_{zz} effect on vibration of multilayered structures. To this purpose a mixed plate model initially introduced by Toledano and Murakami has been extended to dynamics analysis of double curved shells. These models allow both continuous interlaminar transverse shear and normal stresses as well as the zigzag form of the displacement distribution in the shell thickness directions to be modelled. Governing equations have been derived by employing a Reissner's mixed theorem. Classical models on the basis of standard displacement formulations have been considered for comparison purposes. The evaluations of transverse stress effects have been conducted by comparing constant, linear and higher order distributions of transverse displacement components in the plate thickness directions. Free vibrational response of layered, simply supported plates, cylindrical and spherical shells made of isotropic as well as orthotropic layers has been analyzed. The numerical investigation carried out and comparison with earlier results has concluded that:

1. The possibility of describing *a priori* interlaminar continuous transverse normal stress σ_{zz} makes the mixed theories more attractive with respect to other available modelling.
2. Any refinements of classical models are meaningless, unless the effects of interlaminar continuous transverse shear and normal stresses are both taken into account in a multilayered shell theory. © 1999 Academic Press

1. INTRODUCTION

Koiter in his lecture on two-dimensional modelling of traditional isotropic shells [1], based on energy considerations, stated that *a refinement of Love's first approximation theory is indeed meaningless, in general, unless the effects of transverse shear and normal stresses are taken into account at the same time*. More general and systematic substantiation of Koiter's conclusion can be referred to in the books by Goldenvaizer [2] and Cicala [3] in which the the method of asymptotic expansion of the three-dimensional governing equations is employed.

Two-dimensional modellings of multilayered structures (such as laminated constructions, sandwich panels, layered structures used as thermal protection or intelligent structural systems embedding piezo-layers) require amendments to Koiter's recommendation. Among these, the inclusion of continuity of

0022-460X/99/350803 + 27 \$30.00/0 © 1999 Academic Press

displacements – zigzag effects – and of transverse shear and normal stresses – *interlaminar continuity* – at the interface between two adjacent layers are some of the amendments necessary. The role played by zigzag effects and interlaminar continuity has been confirmed by many three-dimensional analyses of layered plates [4–8] and shells [9–14]. Due to the increasing number of parameters (thickness, number of layers and mechanical properties such as the value of the orthotropic ratio of the lamina) the application of asymptotic techniques [15–23] to layered structures has not lead to conclusions as exhaustive as those for the isotropic one layer cases [3]. Among these, the very recent treatments presented by Sutyrin [23] are of particular interest. As far as possible, the shear corrected theories in [23] are derived from variational asymptotic analysis.

Exhaustive overviews on classical and refined models of multilayered structures have been reported in many published review articles. These include the papers by Grigolyuk and Kulikov [24], Kapania and Raciti [25], Kapania [26], Noor *et al.* [27–29] and Soldatos and Timarci [30]. Among the refined theories a convenient distinction can be made between models in which the number of the unknown variables is independent or dependent on the number of the constitutive layers of the shell. Following Reddy [31], we assign the name ESLM (Equivalent Single Layer Models) to the first grouping while LWM (Layer Wise Model) is used to denote the others. Early [32–35] and more recent [36–42] LWMs have shown the superiority of layer-wise approaches over ESL approaches to predict accurately static and dynamic response of thick and very thick structures. The best results have been obtained by mixed LWMs [40–42] which *a priori* describe interlaminar continuous transverse normal stress. On the other hand, LWMs are computationally expensive and the use of ESLMs is preferred in most practical applications. In this paper, attention is restricted to those ESLMs which, according to the Koiter's recommendation, address both transverse shear $\sigma_{\alpha z}$, $\sigma_{\beta z}$ and normal stress σ_{zz} effects.

The work by Hildebrand *et al.*, [43] and by Lo *et al.*, [44] are examples of classical analyses in which higher order displacement models have been employed and σ_{zz} is taken into account. These types of theories do not include interlaminar continuity for the transverse shear and normal stresses nor allow the zigzag form for the displacement variables. On the other hand, transverse normal stress has been discarded in most of the refined ESL analyses [45–51]. In fact, the intrinsic coupling experienced by orthotropic material between in-plane $\sigma_{\alpha\alpha}$, $\sigma_{\beta\beta}$ and out-of-plane σ_{zz} stresses [see equation (3)] makes the *a priori* fulfillment of σ_{zz} interlaminar equilibria difficult. Interlaminar equilibria are usually restricted to the transverse shear components while the zigzag form appears only in the two in-plane components of the displacement. That is, Koiter's recommendation is not taken into account by the latter type of theories.

To allow interlaminar continuous transverse stresses (both shear and normal components) Toledano and Murakami [52], on the basis of a Reissner mixed variational theorem [53], proposed a mixed theory which introduced two independent interlaminar continuous fields for the displacements and transverse stress variables. The displacement field was assumed at a multilayered level while stress variables were considered independent in each layer. The possibility of expressing stress variables in terms of the displacement variables was discussed in reference [54]. Shell applications, which were developed by Bhaskar and Varadan [55] and Jing and Tzeng [56] were restricted to static analysis and neglected σ_{zz}.

In the scenarios above described, the present work has the following aim: to evaluate the effects of σ_{zz} on the vibrational response of plate and shells in cases of both mixed [52] and classical modellings [43]. Such an evaluation would serve to assess the many refined ESLMs which discard σ_{zz}. To this purpose the mixed theory by Toledano and Murakami [52] which had been originally developed for the static analysis of plates, is extended in this paper to dynamic analysis of shells. Related classical models based on the standard displacement formulation are derived for comparison purposes. Transverse stress effect has been evaluated by allowing different polynomials of order N in the assumed expansions of displacement and/or stress unknowns. Further, a layer-wise model which has been shown ([40–42]) to give a quasi-three-dimensional description of multilayered structures is also introduced. This model is used as a reference solution to assess simplified ESLM analyses. All these models are written in this paper in a unified form by referring to techniques developed by the author in earlier works [40–42, 54, 57, 58].

2. PRELIMINARY

The salient features of shell geometry are shown in Figure 1. A laminated shell composed of N_l layers is considered. The integer k, used as superscript or subscript, denotes the layer number which starts from the shell bottom. The layer geometry is denoted by the same symbols as those used for the whole multilayered shell and vice-versa. α_k and β_k are the curvilinear orthogonal co-ordinates (coinciding with principal curvature lines) on the layer reference surface Ω_k (middle surface of the k-layer). z_k denotes the rectilinear co-ordinate in the direction normal to Ω_k. Γ_k is the Ω_k boundary: Γ_k^g and Γ_k^m are those parts of Γ_k on which geometrical and mechanical boundary conditions are imposed, respectively; these boundaries are considered parallel to α_k or β_k. The further dimensionless thickness co-ordinate is introduced, $\zeta_k = 2z_k/h_k$, where h_k denotes the thickness in the A_k domain. The following relation holds for the orthogonal system of curvilinear co–ordinates for the square of line element, for the area of an infinitesimal rectangle on Ω_k, and for an infinitesimal volume, respectively [59]:

$$\begin{aligned} \mathrm{d}s_k^2 &= H_\alpha^k \,\mathrm{d}\alpha_k^2 + H_\beta^k \,\mathrm{d}\beta_k^2 + H_z^k \,\mathrm{d}z_k^2, \\ \mathrm{d}\Omega_k &= H_\alpha^k H_\beta^k \,\mathrm{d}\alpha_k \,\mathrm{d}\beta_k, \\ \mathrm{d}V &= H_\alpha^k H_\beta^k H_z^k \,\mathrm{d}\alpha_k \,\mathrm{d}\beta_k \,\mathrm{d}z_k \end{aligned} \tag{1}$$

where $H_\alpha^k = A^k(1 + z_k/R_\alpha^k)$, $H_\beta^k = B^k(1 + z_k/R_\beta^k)$, $H_z^k = 1$. R_α^k and R_β^k are the radii of curvature in the directions of α_k and β_k respectively. A^k and B^k are the coefficients of the first fundamental form of Ω_k. For the sake of simplicity here attention is

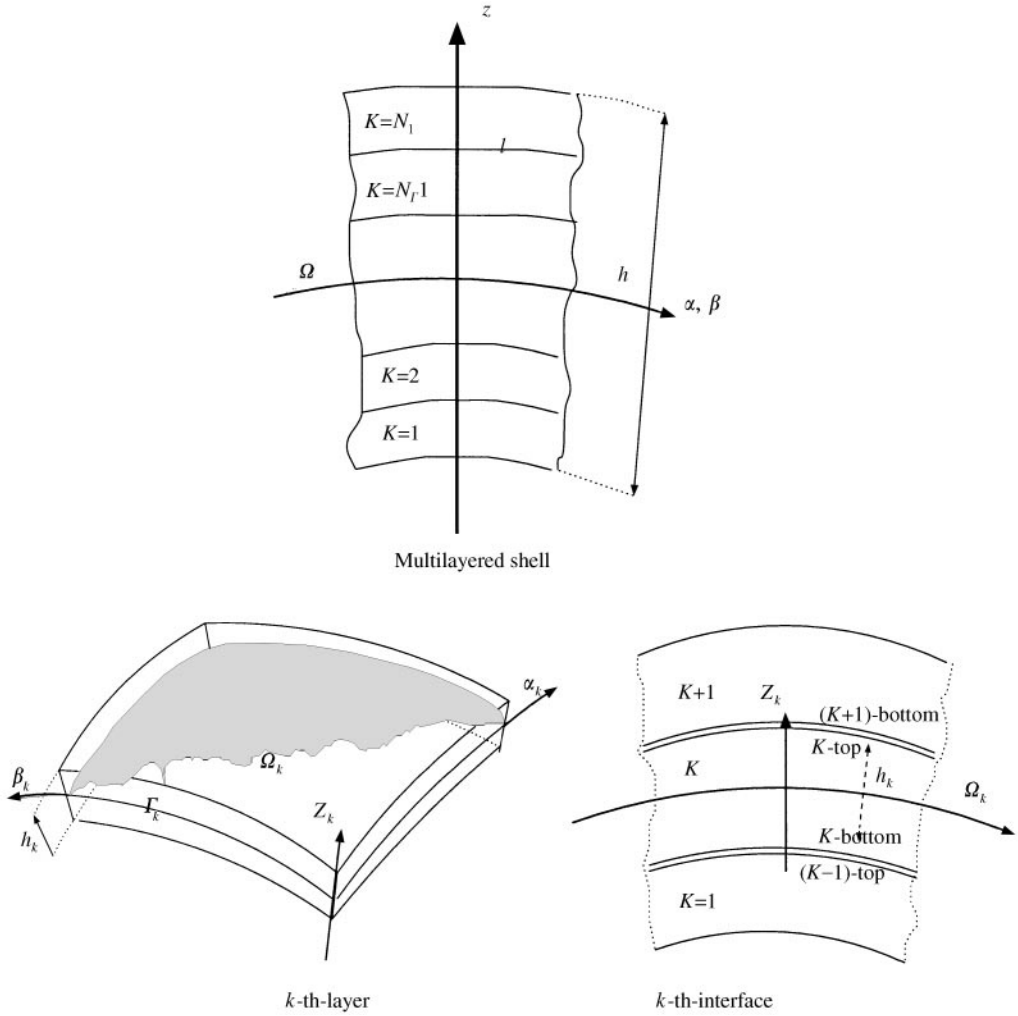

Figure 1. Geometry and notation of multilayered shells.

restricted to a shell with a constant curvature, i.e., double-curved shell (cylindrical, spherical, toroidal geometries) for which $A^k = B^k = 1$.

The laminae are considered to be homogeneous and to operate in the linear elastic range. By employing stiffness coefficients, Hooke's law for the anisotropic k-lamina is written in the form $\sigma_i = \tilde{C}_{ij}\varepsilon_j$ where the sub-indices i and j, ranging from 1 to 6, stand for the index couples $11, 22, 33, 13, 23$ and 12 respectively. The material is assumed to be orthotropic, as specified, by: $\tilde{C}_{14} = \tilde{C}_{24} = \tilde{C}_{34} = \tilde{C}_{64} = \tilde{C}_{15} = \tilde{C}_{25} = \tilde{C}_{35} = \tilde{C}_{65} = 0$. This implies that $\sigma^k_{\alpha z}$ and $\sigma^k_{\beta z}$ depend only on $\varepsilon^k_{\alpha z}$ and $\varepsilon^k_{\beta z}$. In matrix form,

$$\begin{aligned} \boldsymbol{\sigma}^k_{pH_d} &= \tilde{\mathbf{C}}^k_{pp}\boldsymbol{\varepsilon}^k_{pG} + \tilde{\mathbf{C}}^k_{pn}\boldsymbol{\varepsilon}^k_{nG}, \\ \boldsymbol{\sigma}^k_{nH_d} &= \tilde{\mathbf{C}}^k_{np}\boldsymbol{\varepsilon}^k_{pG} + \tilde{\mathbf{C}}^k_{nn}\boldsymbol{\varepsilon}^k_{nG}, \end{aligned} \tag{2}$$

where

$$\tilde{\mathbf{C}}^k_{pp} = \begin{bmatrix} \tilde{C}^k_{11} & \tilde{C}^k_{12} & \tilde{C}^k_{16} \\ \tilde{C}^k_{12} & \tilde{C}^k_{22} & \tilde{C}^k_{26} \\ \tilde{C}^k_{16} & \tilde{C}^k_{26} & \tilde{C}^k_{66} \end{bmatrix}, \qquad \tilde{\mathbf{C}}^k_{pn} = \tilde{\mathbf{C}}^{k^{\mathrm{T}}}_{np} = \begin{bmatrix} 0 & 0 & \tilde{C}^k_{13} \\ 0 & 0 & \tilde{C}^k_{23} \\ 0 & 0 & \tilde{C}^k_{36} \end{bmatrix},$$

$$\tilde{\mathbf{C}}^k_{nn} = \begin{bmatrix} \tilde{C}^k_{44} & \tilde{C}^k_{45} & 0 \\ \tilde{C}^k_{45} & \tilde{C}^k_{55} & 0 \\ 0 & 0 & \tilde{C}^k_{66} \end{bmatrix}.$$

Bold letters denote arrays. The superscript T signifies array transposition. It should be noted that σ_{zz} couples the in-plane and out-of-plane stress and strain components. The subscripts n and p denote transverse (out-of-plane, normal) and in-plane values respectively. Therefore $\boldsymbol{\sigma}^k_p = \{\sigma^k_{\alpha\alpha}, \sigma^k_{\beta\beta}, \sigma^k_{\alpha\beta}\}$, $\boldsymbol{\sigma}^k_n = \{\sigma^k_{\alpha z}, \sigma^k_{\beta z}, \sigma^k_{zz}\}$ and $\boldsymbol{\varepsilon}^k_p = \{\varepsilon^k_{\alpha\alpha}, \varepsilon^k_{\beta\beta}, \varepsilon^k_{\alpha\beta}\}$, $\boldsymbol{\varepsilon}^k_n = \{\varepsilon^k_{\alpha z}, \varepsilon^k_{\beta z}, \varepsilon^k_{zz}\}$. Subscript H denotes stresses evaluated by Hooke's law while subscript G denotes strain from the geometrical relation in equation (4). The sub-subscript d signifies values employed in the displacement formulation. For the mixed solution procedure adopted, the stress–strain relationships are conveniently put in the following mixed form [60]

$$\begin{aligned} \boldsymbol{\sigma}^k_{pH} &= \mathbf{C}^k_{pp}\boldsymbol{\varepsilon}^k_{pG} + \mathbf{C}^k_{pn}\boldsymbol{\sigma}^k_{nM}, \\ \boldsymbol{\varepsilon}^k_{nH} &= \mathbf{C}^k_{np}\boldsymbol{\varepsilon}^k_{pG} + \mathbf{C}^k_{nn}\boldsymbol{\sigma}^k_{nM}, \end{aligned} \tag{3}$$

where both stiffness and compliance coefficients are employed. The subscript M states that the transverse stresses are those of the assumed model (see the next section). The relation between the arrays of coefficients in the two forms of Hooke's law is simply found

$$\begin{aligned} \mathbf{C}^k_{pp} &= \tilde{\mathbf{C}}^k_{pp} - \tilde{\mathbf{C}}^k_{pn}\tilde{\mathbf{C}}^{k^{-1}}_{nn}\tilde{\mathbf{C}}^k_{np}, &\qquad \mathbf{C}^k_{pn} &= \tilde{\mathbf{C}}^k_{pn}\tilde{\mathbf{C}}^{k^{-1}}_{nn}, \\ \mathbf{C}^k_{np} &= -\tilde{\mathbf{C}}^{k^{-1}}_{nn}\tilde{\mathbf{C}}^k_{np}, &\qquad \mathbf{C}^k_{nn} &= \tilde{\mathbf{C}}^{k^{-1}}_{nn}. \end{aligned}$$

Superscript -1 denotes an inversion of the array.

As the model is restricted to the small deformation field, the strain components $\boldsymbol{\varepsilon}^k_p$, $\boldsymbol{\varepsilon}^k_n$ are linearly related to the displacements $\mathbf{u}^k$ ($\mathbf{u}^k = u^k_\alpha, u^k_\beta, u^k_z$), according to the following geometrical relations [59]:

$$\boldsymbol{\varepsilon}^k_{pG} = \mathbf{D}_p\mathbf{u}^k + \mathbf{A}_p\mathbf{u}^k, \qquad \boldsymbol{\varepsilon}^k_{nG} = \mathbf{D}_{n\Omega}\mathbf{u}^k + \mathbf{A}_n\mathbf{u}^k + \mathbf{D}_{nz}\mathbf{u}^k, \tag{4}$$

where

$$\mathbf{D}_p = \begin{bmatrix} \dfrac{\partial_\alpha}{H^k_\alpha} & 0 & 0 \\ 0 & \dfrac{\partial_\beta}{H^k_\beta} & 0 \\ \dfrac{\partial_\beta}{H^k_\beta} & \dfrac{\partial_\alpha}{H^k_\alpha} & 0 \end{bmatrix}, \qquad \mathbf{A}_p = \begin{bmatrix} 0 & 0 & \dfrac{1}{H^k_\alpha R^k_\alpha} \\ 0 & 0 & \dfrac{1}{H^k_\beta R^k_\beta} \\ 0 & 0 & 0 \end{bmatrix},$$

$$\mathbf{D}_{n\Omega} = \begin{bmatrix} 0 & 0 & \dfrac{\partial_\alpha}{H_\alpha^k} \\ 0 & 0 & \dfrac{\partial_\beta}{H_\beta^k} \\ 0 & 0 & 0 \end{bmatrix}, \qquad \mathbf{A}_n = \begin{bmatrix} -\dfrac{1}{H_\alpha^k R_\alpha^k} & 0 & 0 \\ 0 & -\dfrac{1}{H_\beta^k R_\beta^k} & 0 \\ 0 & 0 & 0 \end{bmatrix},$$

$$\mathbf{D}_{nz} = \begin{bmatrix} \partial_z & 0 & 0 \\ 0 & \partial_z & 0 \\ 0 & 0 & \partial_z \end{bmatrix}.$$

No assumption has been made for those terms which are divided by H_α^k and H_β^k are not expanded as Taylor series [57, 59]. That is, curvature terms have been entirely retained in the following developments.

3. DISPLACEMENT AND STRESS ASSUMPTION

3.1. CLASSICAL MODELS

Firstly, classical models are considered. As usual, the displacement variables are expressed in Taylor series in terms of unknown variables which are defined on the plate reference surface Ω,

$$\mathbf{u} = \mathbf{u}_0 + z^r \mathbf{u}_r, \quad r = 1, 2, \ldots, N, \tag{5}$$

where N is a free parameter of the model. Different values for different modellings and different displacement and stress components are assumed. The repeated r indices are summed over their ranges. Subscript 0 denotes displacement values with correspondence to the plate reference surface Ω. Linear and higher order distributions in the z-direction are introduced by the r-polynomials. The assumed models can be written with the same notations that will be adopted for the layer-wise stress model (equation (10)). Equation (5) is therefore rewritten

$$\mathbf{u} = F_t \mathbf{u}_t + F_b \mathbf{u}_b + F_r \mathbf{u}_r = F_\tau \mathbf{u}_\tau, \qquad \tau = t, b, r, \qquad r = 1, 2, \ldots, N-1. \tag{6}$$

Subscript b denotes values related to the plate reference surface Ω ($\mathbf{u}_b = \mathbf{u}_0$) while subscript t refers to the highest term ($\mathbf{u}_t = \mathbf{u}_N$). The F_τ functions assume the following explicit form:

$$F_b = 1, \qquad F_t = z^N, \qquad F_r = z^r, \qquad r = 1, 2, \ldots, N-1. \tag{7}$$

Transverse stress σ_{zz} and strain ε_{zz} effects are discarded by forcing a constant ($N = 0$) distribution for the the u_z-expansion.

3.2. MIXED MODELS

The zigzag form of the displacement fields can be reproduced in equation (5) by employing the Murakami theory [61]. Within the framework of the ESL description and according to references [52, 61] a zigzag term can be introduced into equation (5) (see Figure 2):

$$\mathbf{u}^k = \mathbf{u}_0 + (-1)^k \zeta_k \mathbf{u}_Z + z^r \mathbf{u}_r, \qquad r = 1, 2, \ldots, N. \tag{8}$$

Subscript Z refers to the introduced zigzag term. With unified notations equation (6) becomes

$$\mathbf{u}^k = F_t \mathbf{u}_t + F_b \mathbf{u}_b + F_r \mathbf{u}_r = F_\tau \mathbf{u}_\tau, \qquad \tau = t, b, r, \qquad r = 1, 2, \ldots, N \tag{9}$$

Subscript t refers to the introduced zigzag term ($\mathbf{u}_t = \mathbf{u}_Z$, $F_t = (-1)^k \zeta_k$). It should be noticed that F_t assumes the values ± 1 in correspondence to the bottom and the top interface of the k-layer (see Figure 2).

The thickness expansion used for displacement variables in equation (9) is not suitable for the transverse stress cases. For instance, homogeneous top–bottom plate surface conditions cannot be imposed. Transverse stresses are therefore herein described by means of the layer-wise description [52, 54, 61]:

$$\boldsymbol{\sigma}^k_{nM} = F_t \boldsymbol{\sigma}^k_{nt} + F_b \boldsymbol{\sigma}^k_{nb} + F_r \boldsymbol{\sigma}^k_{nr} = F_\tau \boldsymbol{\sigma}^k_{n\tau}, \qquad \tau = t, b, r,$$
$$r = 2, 3, \ldots, N, \qquad k = 1, 2, \ldots, N_l. \tag{10}$$

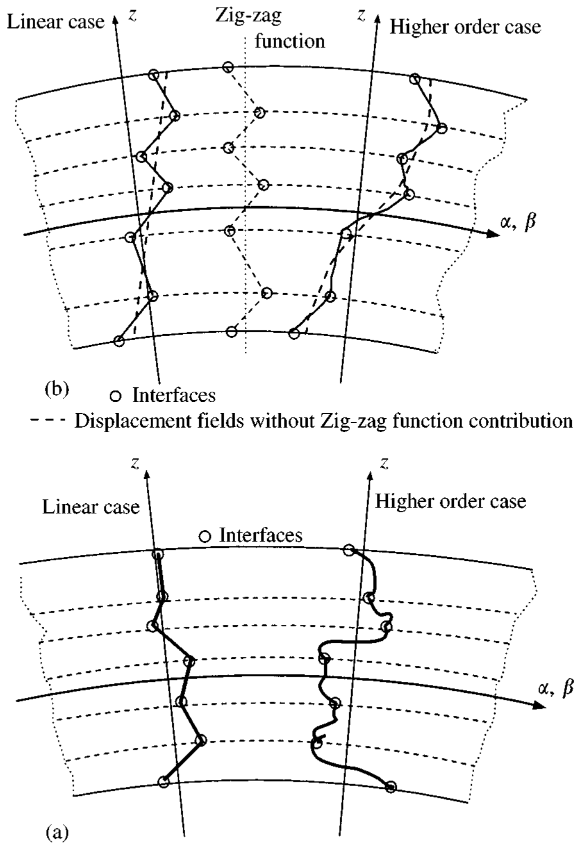

Figure 2. Displacement and stress fields assumed for the employed models. (a) LWM case. (b) ESLM case.

In contrast to equation (9), it is now intended that the subscripts t and b denote values related to the layer top and bottom surface respectively. They consist of the linear part of the expansion. The thickness functions $F_\tau(\zeta_k)$ have now been defined at the k-layer level:

$$F_t = \frac{P_0 + P_1}{2}, F_b = \frac{P_0 - P_1}{2}, \qquad F_r = P_r - P_{r-2}, \qquad r = 2, 3, \ldots, N. \quad (11)$$

in which $P_j = P_j(\zeta_k)$ is the Legendre polynomial of the j-order defined in the ζ_k-domain: $-1 \leqslant \zeta_k \leqslant 1$. The parabolic, cubic and fourth order stress field equation (10) will be associated to linear, parabolic and cubic displacement field in equation (9), respectively, in the numerical investigations. The related polynomials are

$$P_0 = 1, \qquad P_1 = \zeta_k, \qquad P_2 = (3\zeta_k^2 - 1)/2, \qquad P_3 = \frac{5\zeta_k^3}{2} - \frac{3\zeta_k}{2},$$

$$P_4 = \frac{35\zeta_k^4}{8} - \frac{15\zeta_k^2}{4} + \frac{3}{8}$$

The functions selected have the following properties:

$$\zeta_k = \begin{cases} 1: & F_t = 1,\ F_b = 0,\ F_r = 0, \\ -1: & F_t = 0,\ F_b = 1,\ F_r = 0. \end{cases} \quad (12)$$

The top and bottom values have been used as unknown variables. The interlaminar transverse shear and normal stress continuity can therefore be easily linked:

$$\boldsymbol{\sigma}_{nt}^k = \boldsymbol{\sigma}_{nb}^{(k+1)}, \qquad k = 1, N_l - 1. \quad (13)$$

In those cases in which the top/bottom-shell stress values are prescribed (zero or imposed values), the following additional equilibrium conditions must be accounted for:

$$\boldsymbol{\sigma}_{nb}^1 = \bar{\boldsymbol{\sigma}}_{nb}, \qquad \boldsymbol{\sigma}_{nt}^{N_l} = \bar{\boldsymbol{\sigma}}_{nt}, \quad (14)$$

where the over-bar is the imposed value in correspondence to the plate boundary surfaces. Examples of linear and higher order fields have been plotted in Figure 2. The stress variables could be eliminated by employing the *weak form of Hooke's law* proposed in reference [54].

3.3. LAYER-WISE MIXED MODEL

In the author's previous papers [40–42, 54], two independent layer-wise fields are assumed for both displacement and stress variables as in equation (10):

$$\begin{aligned} \mathbf{u}^k &= F_t \mathbf{u}_t^k + F_b \mathbf{u}_b^k + F_r \mathbf{u}_r^k = F_\tau \mathbf{u}_\tau^k, & \tau &= t, b, r, \\ & & r &= 2, 3, \ldots, N, \\ \boldsymbol{\sigma}_{nM}^k &= F_t \boldsymbol{\sigma}^k{}_{nt} + F_b \boldsymbol{\sigma}_{nb}^k + F_r \boldsymbol{\sigma}_{nr}^k = F_\tau \boldsymbol{\sigma}_{n\tau}^k, & k &= 1, 2, \ldots, N_l. \end{aligned} \quad (15)$$

In addition to equation (13) the compatibility of the displacement reads

$$\mathbf{u}_t^k = \mathbf{u}_b^{(k+1)}, \qquad k = 1, N_l - 1. \tag{16}$$

4. GOVERNING EQUATIONS

In order to write all the models mentioned in the previous section it is convenient to refer to all the stress and displacement variables at the k-layer level, i.e. to use a layer-wise description. ESL cases are achieved by writing the governing equations at the multilayered plate level.

The displacement approach is formulated in terms of $\mathbf{u}^k$ by variationally imposing the equilibrium via the principle of virtual displacements. In the dynamic case this establishes

$$\sum_{k=1}^{N_l} \int_{\Omega_k} \int_{A_k} (\delta \boldsymbol{\varepsilon}_{pG}^{k\mathrm{T}} \boldsymbol{\sigma}_{pH_d}^k + \delta \boldsymbol{\varepsilon}_{nG}^{k\mathrm{T}} \boldsymbol{\sigma}_{nH_d}^k)\, \mathrm{d}\Omega_k\, \mathrm{d}z = \sum_{k=1}^{N_l} \int_{\Omega_k} \int_{A_k} \rho^k \delta \mathbf{u}^k \ddot{\mathbf{u}}^k\, \mathrm{d}V + \delta L^e, \tag{17}$$

where δ signifies virtual variations and ρ_k denotes mass density. The variation of the internal work has been split into in-plane and out-of-plane parts and involves the stress obtained from Hooke's Law and the strain from the geometrical relations. δL_e is the virtual variation of the work done by the external layer-forces $\mathbf{p}^k$ $(\{p_x^k, p_y^k, p_z^k\})$.

In the mixed case, the equilibrium and compatibility are both formulated in terms of the $\mathbf{u}^k$ and $\boldsymbol{\sigma}_n^k$ unknowns via Reissner's mixed variational theorem RMVT [53]

$$\sum_{k=1}^{N_l} \int_{\Omega_k} \int_{A_k} (\delta \boldsymbol{\varepsilon}_{pG}^{k\mathrm{T}} \boldsymbol{\sigma}_{pH}^k + \delta \boldsymbol{\varepsilon}_{nG}^{k\mathrm{T}} \boldsymbol{\sigma}_{nM}^k + \delta \boldsymbol{\sigma}_{nM}^{k\mathrm{T}} (\boldsymbol{\varepsilon}_{nG}^k - \boldsymbol{\varepsilon}_{nH}^k))\, \mathrm{d}\Omega_k\, \mathrm{d}z$$
$$= \sum_{k=1}^{N_l} \int_{\Omega_k} \int_{A_k} \rho^k \delta \mathbf{u}^k \ddot{\mathbf{u}}^k\, \mathrm{d}V + \delta L^e.$$

The LHS includes the variations of the internal work in the shell: the first two terms come from the displacement formulation, they will lead to variationally consistent equilibrium conditions, the third "mixed" term variationally enforces the compatibility of the transverse strains components.

4.1. EQUILIBRIUM AND CONSTITUTIVE EQUATIONS FOR THE k-LAYERS: MIXED CASE

In contrast with most of the available shell literature and to the author's previous works related to plates, in the present analysis the definition of stress or strain resultants in the shell thickness direction has been omitted. Such a choice is mainly due to the wish to preserve the terms H_α^k, H_β^k in the strain equation (4). In fact, if the Love's approximation $H_\alpha^k = H_\beta^k = 1$ is not introduced, as is the case in the present article, the definition of stress and strain resultants remains still possible, but according to the author's opinion, not convenient. As a result, together with the derivations of this paper, the governing equations will be directly written in terms of the introduced stress and displacement variables. By using the array formula for the integration by parts similar to those introduced in reference [42] the RMVT work equations equation (18) assumes the following form:

$$\begin{aligned}
&\sum_{k=1}^{N_l}\Bigg(\int_{\Omega_k}\{\delta\mathbf{u}_\tau^{k^{\mathrm{T}}}[(-F_\tau\mathbf{D}_p^{\mathrm{T}}+F_\tau\mathbf{A}_p^{\mathrm{T}})\,\mathbf{C}_{pp}(F_s\mathbf{D}_p+F_s\mathbf{A}_p)\,\mathbf{u}_s^k\\
&\quad+(-F_\tau\mathbf{D}_p^{\mathrm{T}}+F_\tau\mathbf{A}_p^{\mathrm{T}})\,\mathbf{C}_{pn}F_s\boldsymbol{\sigma}_{ns}^k+(-F_\tau\mathbf{D}_{n\Omega}^{\mathrm{T}}+F_\tau\mathbf{A}_n^{\mathrm{T}}+F_{\tau_z})\,F_s\boldsymbol{\sigma}_{ns}^k]\\
&\quad\times\delta\boldsymbol{\sigma}_\tau^{k^{\mathrm{T}}}[(F_\tau F_s\mathbf{D}_{n\Omega}+F_\tau F_s\mathbf{A}_n+F_\tau F_{s_z}-F_\tau\mathbf{C}_{np}(F_s\mathbf{D}_p+F_s\mathbf{A}_p))\,\mathbf{u}_s^k\\
&\quad-F_\tau F_s\mathbf{C}_{nn}\boldsymbol{\sigma}_{ns}^k]\}\,\mathrm{d}\Omega_k+\int_{\Gamma_k}\int_{A_k}\delta\mathbf{u}_\tau^{k^{\mathrm{T}}}[F_\tau\mathbf{I}_p^{\mathrm{T}}\mathbf{C}_{pp}(F_s\mathbf{D}_p+F_s\mathbf{A}_p)\mathbf{u}_s^k\\
&\quad+F_\tau F_s\mathbf{I}_p^{\mathrm{T}}\mathbf{C}_{pn}\boldsymbol{\sigma}_{ns}^k+F_\tau F_s\mathbf{I}_{n\Omega}^{\mathrm{T}}\boldsymbol{\sigma}_{ns}^k]\,\mathrm{d}\Gamma_k\Bigg)\\
&\quad=\sum_{k=1}^{N_l}\int_{\Omega_k}\delta\mathbf{u}_\tau^{k^{\mathrm{T}}}\mathbf{p}_\tau^k\,\mathrm{d}\Omega_k+\sum_{k=1}^{N_l}\int_{\Omega_k}\delta\mathbf{u}_\tau^{k^{\mathrm{T}}}\rho^kF_\tau F_s\ddot{\mathbf{u}}^k\,\mathrm{d}\Omega_k,
\end{aligned}\tag{18}$$

where

$$\mathbf{I}_p=\begin{bmatrix}\dfrac{1}{H_\alpha^k} & 0 & 0\\ 0 & \dfrac{1}{H_\beta^k} & 0\\ \dfrac{1}{H_\beta^k} & \dfrac{1}{H_\alpha^k} & 0\end{bmatrix},\qquad \mathbf{I}_{n\Omega}=\begin{bmatrix}0 & 0 & \dfrac{1}{H_\alpha^k}\\ 0 & 0 & \dfrac{1}{H_\beta^k}\\ 0 & 0 & 0\end{bmatrix}$$

are the variationally consistent load vectors coming from the applied loadings $\mathbf{p}^k$ and $\mathbf{p}_\tau^k=\{p_{x\tau}^k,p_{y\tau}^k,p_{z\tau}^k\}$. The case in which both shearing $(p_{\alpha t}^k,p_{\beta t}^k,p_{\alpha b}^k,p_{\beta b}^k)$ and normal (p_{zt}^k,p_{zb}^k) surface forces are applied could be of practical interest with correspondence to the top and or bottom surface of the layer, $\mathrm{d}\Omega_k^p=\mathrm{d}\Omega_k^t=(1+h_k/2R_\alpha^k)\,(1+h_k/2R_\beta^k)\,\mathrm{d}\Omega_k$ and $\mathrm{d}\Omega_k^p=\mathrm{d}\Omega_k^b=(1-h_k/2R_\alpha^k)\,(1-h_k/2R_\beta^k)\,\mathrm{d}\Omega_k$. By assigning the definition of virtual variations for the unknown stress and displacement variables, the differential system of governing equations and related boundary conditions for the N_l k-layers in each Ω_k domain are found. The equilibrium and compatibility equations are

$$\begin{aligned}
&\delta\mathbf{u}_\tau^k\colon\ \mathbf{K}_{uu}^{k\tau s}\mathbf{u}_s^k+\mathbf{K}_{u\sigma}^{k\tau s}\boldsymbol{\sigma}_{ns}^k=\mathbf{M}^{k\tau s}\ddot{\mathbf{u}}_s^k+\mathbf{p}_\tau^k,\\
&\delta\boldsymbol{\sigma}_{n\tau}^k\colon\ \mathbf{K}_{\sigma u}^{k\tau s}\mathbf{u}_s^k+\mathbf{K}_{\sigma\sigma}^{k\tau s}\boldsymbol{\sigma}_{ns}^k=0
\end{aligned}\tag{19}$$

with boundary conditions

$$\begin{array}{lcl}
\textit{geometrical on } \Gamma_k^g & & \textit{mechanical on } \Gamma_k^m\\
\mathbf{u}_\tau^k=\bar{\mathbf{u}}_\tau^k & \textit{or} & \boldsymbol{\Pi}_u^{k\tau s}\mathbf{u}_s^k+\boldsymbol{\Pi}_\sigma^{k\tau s}\boldsymbol{\sigma}_{ns}^k=\boldsymbol{\Pi}_u^{k\tau s}\bar{\mathbf{u}}_s^k+\boldsymbol{\Pi}_\sigma^{k\tau s}\bar{\boldsymbol{\sigma}}_{ns}^k
\end{array}\tag{20}$$

in which the bar denotes assigned. The introduced differential arrays are given by the following relations:

$$\mathbf{K}_{uu}^{k\tau s} = \int_{A_k} (-F_\tau \mathbf{D}_p^{\mathrm{T}} + F_\tau \mathbf{A}_p^{\mathrm{T}})\, \mathbf{C}_{pp}^k (F_s \mathbf{D}_p + F_s \mathbf{A}_p)\, H_\alpha^k H_\beta^k \,\mathrm{d}z_k,$$

$$\mathbf{K}_{u\sigma}^{k\tau s} = \int_{A_k} [(-F_\tau \mathbf{D}_p^{\mathrm{T}} + F_\tau \mathbf{A}_p^{\mathrm{T}})\, \mathbf{C}_{pn}^k F_s + F_{\tau_z} F_s \mathbf{I} + F_\tau F_s \mathbf{A}_n - F_\tau F_s \mathbf{D}_{n\Omega}^{\mathrm{T}}]\, H_\alpha^k H_\beta^k \,\mathrm{d}z_k,$$

$$\mathbf{K}_{\sigma u}^{k\tau s} = \int_{A_k} \{F_\tau F_s \mathbf{D}_{n\Omega} + F_\tau F_s \mathbf{A}_n + F_\tau F_{s_z} \mathbf{I} - \mathbf{C}_{np}^{k\tau s} (F_\tau F_s \mathbf{D}_p + F_\tau F_s \mathbf{A}_p)\}\, H_\alpha^k H_\beta^k \,\mathrm{d}z_k,$$

$$\mathbf{K}_{\sigma\sigma}^{k\tau s} = -\int_{A_k} F_\tau F_s \mathbf{C}_{nn}^{k\tau s} H_\alpha^k H_\beta^k \,\mathrm{d}z_k, \tag{21}$$

$$\mathbf{\Pi}_u^{k\tau s} = \int_{A_k} F_\tau \mathbf{I}_p^{\mathrm{T}} \mathbf{C}_{pp} (F_s \mathbf{D}_p + F_s \mathbf{A}_p)\, \mathbf{I}_p^{\mathrm{T}} H_\alpha^k H_\beta^k \,\mathrm{d}z_k,$$

$$\mathbf{\Pi}_\sigma^{k\tau s} = \int_{A_k} (F_\tau F_s \mathbf{I}_p^{\mathrm{T}} \mathbf{C}_{pn} + F_\tau F_s \mathbf{I}_{n\Omega}^{\mathrm{T}})\, H_\alpha^k;\; H_\beta^k \,\mathrm{d}z_k,$$

$$\mathbf{M}^{k\tau s} = \int_{A_k} \rho^k F_\tau F_s \mathbf{I}\, H_\alpha^k H_\beta^k \,\mathrm{d}z_k.$$

$\mathbf{I}$ is the unit array. As usual in two-dimensional modellings, the integration in the thickness direction can be made *a priori* by introducing the following layer integrals (the further integrals related to the displacement formulation (see next section) are introduced also);

$$\begin{aligned}
(J^{k\tau s}, J_\alpha^{k\tau s}, J_\beta^{k\tau s}, J_{\alpha/\beta}^{k\tau s}, J_{\beta/\alpha}^{k\tau s}, J_{\alpha\beta}^{k\tau s}) &= \int_{A_k} F_\tau F_s \left(1, H_\alpha^k, H_\beta^k, \frac{H_\alpha^k}{H_\beta^k}, \frac{H_\beta^k}{H_\alpha^k}, H_\alpha^k H_\beta^k\right) \mathrm{d}z,\\
(J^{k\tau_z s}, J_\alpha^{k\tau_z s}, J_\beta^{k\tau_z s}, J_{\alpha\beta}^{k\tau_z s}) &= \int_{A_k} F_{\tau_z} F_s (1, H_\alpha^k, H_\beta^k, H_\alpha^k H_\beta^k)\, \mathrm{d}z,\\
(J^{k\tau s_z}, J_\alpha^{k\tau s_z}, J_\beta^{k\tau s_z}, J_{\alpha\beta}^{k\tau s_z}) &= \int_{A_k} F_\tau F_{s_z} (1, H_\alpha^k, H_\beta^k, H_\alpha^k H_\beta^k)\, \mathrm{d}z,\\
(J^{k\tau_z s_z}, J_{\alpha\beta}^{k\tau_z s_z}) &= \int_{A_k} F_{\tau_z} F_{s_z} (1, H_\alpha^k H_\beta^k)\, \mathrm{d}z.
\end{aligned} \tag{22}$$

As a further step, the differential and algebraic operators can be conveniently split in the two terms related to the H_α^k and H_α^k, respectively,

$$(\mathbf{D}_p, \mathbf{A}_p, \mathbf{D}_{n\Omega}, \mathbf{A}_n, \mathbf{I}_p, \mathbf{I}_{n\Omega}) = \frac{1}{H_\alpha} (\mathbf{D}_p^\alpha, \mathbf{A}_p^\alpha, \mathbf{D}_{n\Omega}^\alpha, \mathbf{A}_n^\alpha, \mathbf{I}_p, \mathrm{I}_{n\Omega})$$

$$+ \frac{1}{H_\beta} (\mathbf{D}_p^\beta, \mathbf{A}_p^\beta, \mathbf{D}_{n\Omega}^\beta, \mathbf{A}_n^\beta, \mathbf{I}_p^\beta, \mathbf{I}_{n\Omega}^\beta). \tag{23}$$

Therefore, the differential operators of equations (21) are written

$$
\begin{aligned}
\mathbf{K}_{uu}^{k\tau s} &= (-\mathbf{D}_p^{\alpha\mathrm{T}} + \mathbf{A}_p^{\alpha\mathrm{T}})\mathbf{C}_{pp}[J_{\beta/\alpha}^{k\tau s}(\mathbf{D}_p^{\alpha} + \mathbf{A}_p^{\alpha}) + J^{k\tau s}(\mathbf{D}_p^{\beta} + \mathbf{A}_p^{\beta})] \\
&\quad + (-\mathbf{D}_p^{\beta\mathrm{T}} + \mathbf{A}_p^{\beta\mathrm{T}})\mathbf{C}_{pp}[J_{\alpha/\beta}^{k\tau s}(\mathbf{D}_p^{\alpha} + \mathbf{A}_p^{\alpha}) + J^{k\tau s}(\mathbf{D}_p^{\beta} + \mathbf{A}_p^{\beta})], \\
\mathbf{K}_{u\sigma}^{k\tau s} &= (-J_{\beta}^{k\tau s}\mathbf{D}_p^{\alpha^{\mathrm{T}}} - J_{\alpha}^{k\tau s}\mathbf{D}_p^{\beta^{\mathrm{T}}} + J_{\alpha}^{k\tau s}\mathbf{A}_p^{\beta^{\mathrm{T}}} + J_{\beta}^{k\tau s}\mathbf{A}_p^{\alpha^{\mathrm{T}}})\,\mathbf{C}_{pn}^{k} \\
&\quad + J_{\alpha\beta}^{k\tau_z s}\mathbf{I} + (J_{\beta}^{k\tau s}\mathbf{A}_n^{\alpha\mathrm{T}} + J_{\alpha}^{k\tau s}\mathbf{A}_n^{\beta\mathrm{T}}) - J_{\beta}^{k\tau s}\mathbf{D}_{n\Omega}^{\alpha\mathrm{T}} - J_{\alpha}^{k\tau s}\mathbf{D}_{n\Omega}^{\beta\mathrm{T}}, \\
\mathbf{K}_{\sigma u}^{k\tau s} &= -\mathbf{C}_{np}^{k}(J_{\beta}^{k\tau s}\mathbf{D}_p^{\alpha} + J_{\alpha}^{k\tau s}\mathbf{D}_p^{\beta} + J_{\alpha}^{k\tau s}\mathbf{A}_p^{\beta} + J_{\beta}^{k\tau s}\mathbf{A}_p^{\alpha}) \\
&\quad + J_{\alpha\beta}^{k\tau s_z}\mathbf{I} + (J_{\beta}^{k\tau s}\mathbf{A}_n^{\alpha} + J_{\alpha}^{k\tau s}\mathbf{A}_n^{\beta}) + J_{\beta}^{k\tau s}\mathbf{D}_{n\Omega}^{\alpha} + J_{\alpha}^{k\tau s}\mathbf{D}_{n\Omega}^{\beta}, \\
\mathbf{K}_{\sigma\sigma}^{k\tau s} &= -J_{\alpha_\beta}^{k\tau s}\mathbf{C}_{nn}^{k\tau s}, \\
\mathbf{\Pi}_{u}^{k\tau s} &= (J_{\beta/\alpha}^{k\tau s}\mathbf{I}_p^{\alpha\mathrm{T}} + J^{k\tau s}\mathbf{I}_p^{\beta\mathrm{T}})\mathbf{C}_{pp}(\mathbf{D}_p^{\alpha} + \mathbf{A}_p^{\alpha}) + (J^{k\tau s}\mathbf{I}_p^{\alpha\mathrm{T}} + J_{\alpha/\beta}^{k\tau s}\mathbf{I}_p^{\beta\mathrm{T}})\mathbf{C}_{pp}(\mathbf{D}_p^{\beta} + \mathbf{A}_p^{\beta}), \\
\mathbf{\Pi}_{\sigma}^{k\tau s} &= (J_{\beta}^{k\tau s}\mathbf{I}_p^{\alpha\mathrm{T}} + J_{\alpha}^{k\tau s}\mathbf{I}_p^{\beta\mathrm{T}})\,\mathbf{C}_{pn} + J_{\beta}^{k\tau s}\mathbf{I}_{n\Omega}^{\alpha\mathrm{T}} + J_{\alpha}^{k\tau s}\mathbf{I}_{n\Omega}^{\beta\mathrm{T}}.
\end{aligned}
\tag{24}
$$

The inertia array is found as

$$
\mathbf{M}_{ij}^{k\tau s} = J_{\alpha\beta}^{k\tau s}\delta_{ij}, \quad i, j = 1, 3, \tag{25}
$$

where the Kroneker symbol δ_{ij} has been introduced. Cylindrical shell equations are simply obtained by enforcing $R_\alpha = \infty$ (or $R_\beta = \infty$) while spherical shell geometries correspond to the case $R_\alpha = R_\beta$. Neglecting all the curvature terms the governing equation written for multilayered plates [40] are given as particular cases.

Explicit forms of the governing equations for each layer can be written by expanding the introduced subscripts and superscripts in the previous arrays as follows:

$$
k = 1, 2, \ldots, N_l, \quad \tau = t, r, b, \quad s = t, r, b, (r = 2, \ldots, N).
$$

4.2. EQUILIBRIUM EQUATIONS FOR THE k-LAYERS: CLASSICAL DISPLACEMENT FORMULATIONS

Upon introducing equations (3), (6), and (4) and following the same procedure developed for the mixed case, (equation (17)) leads to

$$
\begin{aligned}
&\sum_{k=1}^{N_l}\Bigg(\int_{\Omega_k}\int_{A_k} \delta\mathbf{u}_\tau^{k^{\mathrm{T}}}\{(-F_\tau\mathbf{D}_p^{\mathrm{T}} + F_\tau\mathbf{A}_p^{\mathrm{T}})\,[\tilde{\mathbf{C}}_{pp}(F_s\mathbf{D}_p + F_s\mathbf{A}_p) \\
&\quad + \tilde{\mathbf{C}}_{pp}(F_s\mathbf{D}_{n\Omega} + F_s\mathbf{A}_n + F_{s_z})] + (-F_\tau\mathbf{D}_{n\Omega}^{\mathrm{T}} + F_\tau\mathbf{A}_n^{\mathrm{T}} + F_{\tau_z}) \\
&\quad \times [\tilde{\mathbf{C}}_{np}(F_s\mathbf{D}_p + F_s\mathbf{A}_p) + \tilde{\mathbf{C}}_{nn}(F_s\mathbf{D}_{n\Omega} + F_s\mathbf{A}_n + F_{s_z})]\}\,\mathbf{u}_s\,\mathrm{d}\Omega_k \\
&\quad + \int_{\Gamma_k}\int_{A_k} \delta\mathbf{u}_\tau^{k^{\mathrm{T}}}\{F_\tau\mathbf{I}_p^{\mathrm{T}}[\tilde{\mathbf{C}}_{pp}(F_s\mathbf{D}_p + F_s\mathbf{A}_p) + \tilde{\mathbf{C}}_{pp}(F_s\mathbf{D}_{n\Omega} + F_s\mathbf{A}_n + F_{s_z})] \\
&\quad + F_\tau\mathbf{I}_{n\Omega}^{\mathrm{T}}[\tilde{\mathbf{C}}_{np}(F_s\mathbf{D}_p + F_s\mathbf{A}_p) + \tilde{\mathbf{C}}_{nn}(F_s\mathbf{D}_{n\Omega} + F_s\mathbf{A}_n + F_{s_z})]\}\,\mathbf{u}_s\,\mathrm{d}\Gamma_k\Bigg) \\
&\quad = \sum_{k=1}^{N_l}\int_{\Omega_k}\delta\mathbf{u}_\tau^{k^{\mathrm{T}}}\mathbf{p}_\tau^{k}\,\mathrm{d}\Omega_k^{p} + \sum_{k=1}^{N_l}\int_{\Omega_k}\delta\mathbf{u}_\tau^{k^{\mathrm{T}}}\rho^k F_\tau F_s\ddot{\mathbf{u}}^{k}.
\end{aligned}
\tag{26}
$$

The differential system of governing equations and related boundary conditions are as follows:

$$\begin{array}{lll} \delta\mathbf{u}_\tau^k: & & \mathbf{K}_d^{k\tau s}\mathbf{u}_s^k = \mathbf{M}^{k\tau s}\ddot{\mathbf{u}}_s^k + \mathbf{p}_\tau^k \\ \textit{geometrical on } \Gamma_k^g & & \textit{mechanical on } \Gamma_k^m \\ \mathbf{u}_\tau^k = \bar{\mathbf{u}}_\tau^k & \textit{or} & \mathbf{\Pi}_d^{k\tau s}\mathbf{u}_s^k = \mathbf{\Pi}_d^{k\tau s}\bar{\mathbf{u}}_s^k. \end{array} \tag{27}$$

The introduced differential arrays are

$$\begin{aligned} \mathbf{K}_d^{k\tau s} = \int_{A_k} \{(-F_\tau \mathbf{D}_p^{\mathrm{T}} + F_\tau \mathbf{A}_p^{\mathrm{T}})[\tilde{\mathbf{C}}_{pp}(F_s\mathbf{D}_p + F_s\mathbf{A}_p) \\ + \tilde{\mathbf{C}}_{pn}(F_s\mathbf{D}_{n\Omega} + F_s\mathbf{A}_n + F_{s_z})] + (-F_\tau\mathbf{D}_{n\Omega}^{\mathrm{T}} + F_\tau\mathbf{A}_n^{\mathrm{T}} + F_{\tau_z}) \\ \times[\tilde{\mathbf{C}}_{np}(F_s\mathbf{D}_p + F_s\mathbf{A}_p) + \tilde{\mathbf{C}}_{nn}(F_s\mathbf{D}_{n\Omega} + F_s\mathbf{A}_n + F_{s_z})]\}\, H_\alpha^k H_\beta^k \,\mathrm{d}z_k, \end{aligned} \tag{28}$$

$$\begin{aligned} \mathbf{\Pi}_d^{k\tau s} = \int_{A_k} \{F_\tau \mathbf{I}_p^{\mathrm{T}}[\tilde{\mathbf{C}}_{pp}(F_s\mathbf{D}_p + F_s\mathbf{A}_p) + \tilde{\mathbf{C}}_{pp}(F_s\mathbf{D}_{n\Omega} + F_s\mathbf{A}_n + F_{s_z})] \\ + F_\tau\mathbf{I}_{n\Omega}^{\mathrm{T}}[\tilde{\mathbf{C}}_{np}(F_s\mathbf{D}_p + F_s\mathbf{A}_p) + \tilde{\mathbf{C}}_{nn}(F_s\mathbf{D}_{n\Omega} + F_s\mathbf{A}_n + F_{s_z})]\}\, H_\alpha^k H_\beta^k \,\mathrm{d}z_k. \end{aligned}$$

The definitions given by equations (22) and (23) can be introduced in the previous arrays in a manner similar to that for the mixed case. For the sake of brevity the resulting formula are not given.

4.3. ASSEMBLY FROM LAYER TO MULTILAYERED LEVEL

In the previous sections mixed and standard displacement formulations have been written for the N_l independent layers. Multilayered equations can be written according to the usual variational statements; stiffness and/or compliances related to the same variables are accumulated in this process. Interlaminar continuity conditions are imposed at this stage. Details on this procedure can be found in the papers mentioned earlier. Multilayered arrays are introduced at the very end of the assemblage. The equilibrium and boundary conditions for the displacement formulation take the following form:

$$\begin{array}{ll} \mathbf{K}_d\mathbf{u} = \mathbf{M}\ddot{\mathbf{u}} + \mathbf{p}, & \\ \mathbf{u} = \bar{\mathbf{u}} & \text{or } \mathbf{\Pi}_d\mathbf{u} = \mathbf{\Pi}_d\bar{\mathbf{u}} \end{array} \tag{29}$$

while for the mixed case, one has

$$\begin{aligned} \mathbf{K}_{uu}\mathbf{u} + \mathbf{K}_{u\sigma}\boldsymbol{\sigma}_n &= \mathbf{M}\ddot{\mathbf{u}} + \mathbf{p} + \mathbf{p}_u^{1N_l}, \\ \mathbf{K}_{\sigma u}\mathbf{u} + \mathbf{K}_{\sigma\sigma}\boldsymbol{\sigma}_n &= \mathbf{p}_\sigma^{1N_l} \end{aligned} \tag{30}$$

while the boundary conditions are

$$\mathbf{u} = \bar{\mathbf{u}} \quad \text{or} \quad \mathbf{\Pi}_u\mathbf{u} + \mathbf{\Pi}_\sigma\boldsymbol{\sigma}_n = \mathbf{\Pi}_u\bar{\mathbf{u}} + \mathbf{\Pi}_\sigma\bar{\boldsymbol{\sigma}}_n + \mathbf{q}_\sigma^{1N_l}, \tag{31}$$

$\mathbf{p}_u^{1N_l}$ and $\mathbf{p}_\sigma^{1N_l}$ are the arrays obtained from the transverse stress values imposed at the top/bottom of the plate.

4.4. CLOSED-FORM SOLUTIONS

The boundary value problem governed by equations (29), (30) and (31) in the most general case of geometry, boundary conditions and lay-outs, could be solved by implementing only approximate solution procedures. In order to assess the proposed models these equations are solved for a special case in which closed-form solutions are given. The particular case in which the material has the following properties (as it is the case of cross-ply shells) $\tilde{C}_{16} = \tilde{C}_{26} = \tilde{C}_{36} = \tilde{C}_{45} = 0$ has been considered, for which Navier-type closed-form solutions can be found by assuming the following harmonic forms for the applied loadings $\mathbf{p}^k = \{p^k_{\alpha_\tau}, p^k_{\beta_\tau}, p^k_{z_\tau}\}$ and unknown displacement $\mathbf{u}^k = \{u^k_{\alpha_\tau}, u^k_{\beta_\tau}, u^k_{z_\tau}\}$ and stress $\boldsymbol{\sigma}^k_n = \{\sigma^k_{\alpha z_\tau}, \sigma^k_{\beta z_\tau}, \sigma^k_{zz_\tau}\}$ variables in each k-layer:

$$\begin{aligned}
(u^k_{\alpha_\tau}, \sigma^k_{\alpha z_\tau}, p^k_{\alpha_\tau}) &= \sum_{m,n} (U^k_\alpha, S^k_{\alpha z_\tau}, P^k_{\alpha_\tau}) \cos\frac{m\pi\alpha_k}{a_k} \sin\frac{n\pi\beta_k}{b_k} \mathrm{e}^{i\omega_{mn}\hat{t}}, \quad k = 1, N_l,\\
(u^k_{\beta_\tau}, \sigma^k_{\beta z_\tau}, p^k_{\beta_\tau}) &= \sum_{m,n} (U^k_\beta, S^k_{\beta z_\tau}, P^k_{\beta_\tau}) \sin\frac{m\pi\alpha_k}{a_k} \cos\frac{n\pi\beta_k}{b_k} \mathrm{e}^{i\omega_{mn}\hat{t}}, \quad \tau = t, b, r, \qquad (32)\\
(u^k_{z_\tau}, \sigma^k_{zz_\tau}, p^k_{z_\tau}) &= \sum_{m,n} (U^k_z, S^k_{zz_\tau}, P^k_{z_\tau}) \sin\frac{m\pi\alpha_k}{a_k} \sin\frac{n\pi\beta_k}{b_k} \mathrm{e}^{i\omega_{mn}\hat{t}}, \quad r = 2, N
\end{aligned}$$

which correspond to simply supported boundary conditions. a_k and b_k are the shell lengths in the α_k and β_k directions, respectively, while m and n are the corresponding wave numbers; $i = \sqrt{-1}$, $\hat{t}$ is the time and ω_{mn} is the circular frequency. Capital letters at the RHS denote corresponding maximum amplitudes. Upon substitution of equation (32) the governing equations assume the form of a linear system of ordinary differential equations in the time domain. The free vibration response leads to an eigenvalue problem. Upon elimination of the stress unknowns, the mixed case leads to

$$||\hat{\mathbf{K}}_{uu} - (\hat{\mathbf{K}}_{u\sigma}(\hat{\mathbf{K}}_{\sigma\sigma})^{-1}\hat{\mathbf{K}}_{\sigma u}) - \omega^2_{mn}\hat{\mathbf{M}}|| = 0. \qquad (33)$$

The double bar denotes determinant, while the hat indicates arrays constituted by real numbers. This procedure has been coded for the different case theories and results are discussed in the next section.

5. RESULTS AND DISCUSSION

The two-dimensional theories derived above have been applied to a large number of homogeneous and layered, simply supported, plates and cylindrical and spherical shell problems. The most significant results are described in the following analysis. Generally, the free vibrational response has been analyzed and compared to three-dimensional solutions as well as to available refined theories. A compendium of the acronyms used to denote the theories considered have been given in Table 1. Continuous reference to these acronyms is made in the subsequent text.

As a preliminary assessment Tables 2–4 compare the proposed models to available mixed results. Thin and thick as well as square and rectangular plate

TABLE 1

List of the acronyms used to denote plate and shell theories

— *Theories from literature*	
CLT	Classical Lamination Theory
FSDT	First order Shear Deformation Theory
ESLM	Equivalent Single Layer Model
C&P1, C&P3	Linear and cubic case after Cho and Parmerter [49]
D&P	Dennis and Palazotto [62]
D&S1, D&S3	Linear and cubic case after Di Sciuva [63]
IK&T	Idlbi, Karama and Touratier [51]
J&T	Jing and Tzeng [56]
LC&W	Lo, Christiansen and Wu [44]
Mur.	Murakami [61]
PAR_{ds}, HYP_{ds}, UNI_{cs}, PAR_{cs}, HYP_{ds}	Timarci and Soldatos [50]
R&L	Reddy and Liu [64]
R&P	Reddy and Phan [65]
Ren	Ren [48]
T&M3	Toledano and Murakami [52]
ZZL	Di Sciuva and Carrera [66]
LWM	Layer Wise Model
LWM-1	Cho *et al.* [37]
LWM-2	Nosier *et al.* [38]
— *Present Theories*	
D1d, D2d, D3d†	Classical models discarding σ_{zz}
D1i, D2i, D3i‡	Classical models in equations (5)
M1i, M2i, M3i	Mixed models in equations (9), (10)
M1d, M2d, M3d	Mixed models discarding σ_{zz}
LW4	Mixed layer-wise model equation (15) relate to $N = 4$

† 1,2,3 denote linear, parabolic and cubic u-fields, respectively, while d signifies that σ_{zz} has been discarded.
‡ i denotes results including σ_{zz}.

geometries have been analyzed. Cross-ply, symmetrically ($N_l = 3, 9$) and unsymmetrically ($N_l = 4$) laminated plates are considered in Tables 2 and 3 and Figure 3. The mechanical data of the lamina are those used by Pagano [5]: $E_L/E_T = 25 \times 10^6$ psi, $G_{LT}/E_T = 0{\cdot}5 \times 10^6$ psi, $G_{TT}/E_T = 0{\cdot}2 \times 10^6$ psi, $\nu_{LT} = \nu_{TT} = 0{\cdot}25$, where, following the usual notation [31], L signifies the fiber direction, T the transverse direction and ν_{LT} is the major Poisson ratio. A good agreement with the mixed models by Murakami [61] and Toledano and Murakami [52] has been found. Further, the LW4 analysis matches the exact solution with excellent accuracy. This result confirms [40–42] the reliability of layer-wise mixed models to give a three- dimensional description of stress and displacement fields in laminated plates. LW4 analysis has in fact been taken as a reference solution in the present work wherever three-dimensional solution are not available. The improvements introduced by taking σ_{zz} effects into account are evident for the thick plate cases.

TABLE 2

Maximum transverse displacement $\bar{U}_z = U_z \times 100E_T h^3/(p_{z_t}^{N_l} a^4)$ $(z = 0)$ of thick plate in cylindrical bending. Comparison of present analyses to exact solutions by Pagano [5] and to available mixed results

	$a/h = 4$		$a/h = 6$	
	$N_l = 3$	$N_l = 4$	$N_l = 3$	$N_l = 4$
Exact	2·887	4·181	1·635	2·556
T&M3	2·881	4·105	1·634	2·519
C&P3	—	4·083	—	2·501
Mur.	2·907	3·316	1·636	2·107
C&P1	—	3·316	—	2·107
LC&W	2·687	3·587	1·514	2·242
Present analysis				
LW4	2·887	4·181	1·625	2·556
— σ_{zz} included				
M3i	2·881	4·102	1·634	2·514
M2i	2·831	3·478	1·602	2·195
M1i	2·904	3·300	1·634	2·095
— σ_{zz} discarded				
M3d	2·898	4·124	1·637	2·516
M2d	2·848	3·488	1·605	2·195
M1d	2·904	3·306	1·634	2·098

TABLE 3

Influence of thickness ration on $\bar{U}_z = U_z \times 100E_T h^3/(p_{z_t}^{N_l} a^4)$ $(z = 0)$ and $\bar{S}_{xz} = S_{xz}/(p_{z_t}^{N_l} a/h)$, ($z = 0$ unless denoted). Rectangular ($b = 3a$) three-layered plates. Exact solution by Pagano [5]

	$\bar{U}_z$			$\bar{S}_{xz}$			
a/h	4	10	20	4	z	10	20
Exact	2·820	0·919	0·610	0·387	—	0·420	0·434
IK&T	2·729	0·918	0·609	0·378	—	0·441	0·451
D&S1	2·717	0·881	0·599	0·366	—	0·419	—
D&S3	2·757	0·919	0·610	0·329	—	0·420	—
Ren	2·80	0·920	—	0·317	—	0·415	—
Present analysis							
LW4	2·821	0·919	0·610	0·387	− 0·23	0·420	0·434
— σ_{zz} included							
M3i	2·815	0·919	0·609	0·385	− 0·23	0·420	0·434
M2i	2·767	0·906	0·606	0·393	− 0·23	0·421	0·435
M1i	2·839	0·915	0·606	0·399	− 0·23	0·420	0·434
D3i	2·625	0·867	0·596	0·378	− 0·17	0·427	0·436
— σ_{zz} discarded							
M3d	2·832	0·918	0·607	0·386	± 0·27	0·420	0·434
M2d	2·784	0·904	0·604	0·393	± 0·23	0·421	0·435
M1d	2·839	0·915	0·606	0·394	± 0·23	0·420	0·434
D3d	2·644	0·866	0·593	0·377	0	0·427	0·436

TABLE 4

Ren's shells problem. Symmetric three layers 90/0/90. *Transverse displacement amplitude.* $\bar{U}_z = U_z \times 10E_T h^3/P^1_{z_b} R^4_\beta$, $z = 0$. *Exact solution by Ren* [9]

R_β/h	2	4	10	50
Exact	1·436	0·457	0·144	0·0808
CLT	0·0799	0·0781	0·0777	0·0776
FSDT	—	0·342	0·120	0·0793
D&P	1·141	0·382	0·128	0·0796
J&T	—	0·459	0·142	0·0802
Present analysis				
LW4	1·432	0·4580	0·1440	0·0808
— σ_{zz} included				
M3i	1·412	0·4535	0·1440	0·0808
M1i	1·474	0·4569	0·1432	0·0805
D3i	1·364	0·4225	0·1363	0·0805
D1i	1·112	0·3292	0·1187	0·0795
— σ_{zz} discarded				
M3d	1·454	0·4583	0·1428	0·0804
M1d	1·464	0·4595	0·1423	0·0804
D3d	1·402	0·4271	0·1351	0·0802
D1d	1·159	0·3314	0·1179	0·0795

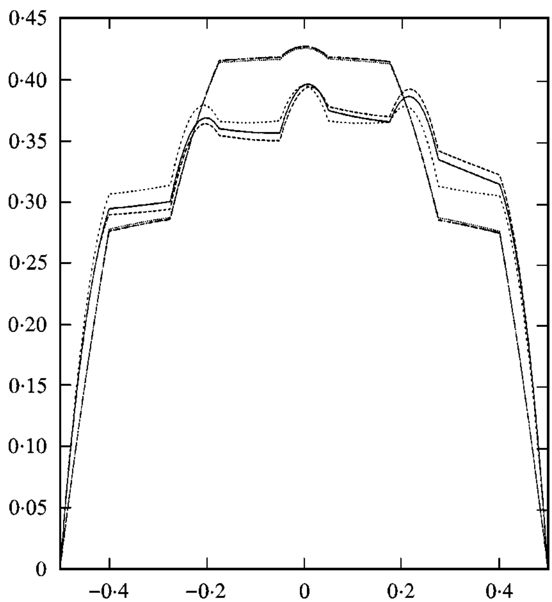

Figure 3. $S_{xz}/(p^{N_l}_{z_t} a/h)$ versus z. Cross-ply, square plate. Data of Table 2 (nine layers case, $a/h = 2{\cdot}5$, 100). LW-2·5 —; M3i-2.5 ----; M3d-2·5 ····; LW4-10 ········; M3i-10 ---·--; M3d-10 --·-·---.

Higher order mixed models lead to the best description. A comparison with the other models of Table 3 (C&P1, C&P3, D&S1, D&S3, IK&T which allow interlaminar continuous transverse shear stresses) reveals that the extension of such a continuity to σ_{zz} permits one to conclude that the M3i-model leads to the best ESL results. These comments are further confirmed by comparing the M3d,M2d,M1d to M3i,M2i, M1i analysis. Figure 3 makes evident a fundamental limitation of each laminated theory which neglected σ_{zz}. (i) The plate has been loaded at the top surface: LW4 and M3i analyses show that σ_{zz} enforces a non-symmetrical distribution of transverse shear stress $\bar{S}_{xz}$ versus z. (ii) The plate in symmetrically laminated M3d analysis (as well as any other plate theories in which σ_{zz} is discarded) *tragically* leads to a symmetrical distribution of $\bar{S}_{xz}$ versus z. (iii) It is concluded that analyses which discard σ_{zz} cannot improve the transverse shear stress fields in the whole thickness. It should be further noticed that the maximum value $(S_{xz}/p_{z_t}^{N_l})_{\max} \approx 0{\cdot}4 \times 2{\cdot}5 \approx 1$ is almost coincident to the maximum σ_{zz} value $(S_{zz}/p_{z_t}^{N_l})_{\max} = 1$ for the thicker plate case; this is for the simple reason (as stated by Koiter, see Section 1) that σ_{zz} cannot be neglected in thick plate analysis. Symmetry is reached for thinner plates. Additional results of σ_{zz} effects on static analysis of multilayered plates has been provided by the author in reference [58].

A cross-ply laminated cylindrical panel, loaded by harmonic distribution of transverse pressure of amplitude $P_{z_t}^1$, applied at the bottom external surface has been considered in Table 4. Exact solutions were given by Ren [9]. A comparison on transverse displacement amplitude has been made with results by Jing and Tzeng [56] that applied the Reissner's theorem in conjunction to a linear trough the thickness displacement fields. Comments made above for the plate geometry can be confirmed for the cylindrical shell panel case.

Free vibration response of isotropic and cross-plied plates and cylindrical shells is considered in Tables 5–10. Analyses in which σ_{zz} is discarded (M3d results) overestimate the vibration response with respect to M3i case. Higher order frequencies related to higher modes are considered in Table 5 for an isotropic plate. It is shown that the influence of σ_{zz} is very much subordinate to the vibrational modes. In particular, the first thickness-twist mode seems not to be affected by refinements introduced in the two-dimensional modellings considered. It should be noted that the higher order theories D3d can lead to poorer results than D2i and D1i. This result confirms Koiter's recommendation [1]. Zigzag and interlaminar continuity are not applicable to this problem. Mixed results, are in fact not given.

Table 6 compares the present results with those by Nosier *et al.* [38] for a four-layered cross-ply plate. Fundamental and higher frequencies related to two half-waves modes are considered for a symmetrically cross-ply laminated plate. LW4 accuracy with respect to exact solution is confirmed. Only nine frequencies can be found for the D3d analysis. M3i analysis leads to the best ESLM description. It is to be noted that M3d results can be better or worst than D3i ones; it is not predictable *a priori* whether refinements of classical theories discarding σ_{zz} (such as M3d case) will improve classical analysis (such as M3i case) including σ_{zz}.

A comparison to the recent exact solution by Ye and Soldatos [14] and to several refined models quoted in reference [50] has been provided in Table 7. A three-layered, moderately thick cylindrical shell has been considered. Good

TABLE 5

Comparison of present analysis to exact by Srinivas and alii [6] *and to other refined models on the lowest five circular frequency parameter* $\omega h\sqrt{\rho/G}$. *Simply supported square isotropic plates* ($\nu = 0{\cdot}3$). A *and* S *denote modes which are antisymmetric and symmetric about the mid-plane.* I–S *and* II–S *are both thickness-twist modes*

Model	I–A	I–S	II–S	II–A	III–A
			$mh/a = 0{\cdot}1$, $nh/a = 0{\cdot}1$		
Exact	0·0931	0·4443	0·7498	3·1729	3·2465
LWM-1	0·0931	0·4443	0·7499	3·1736	3·2496
R&P	0·0931	—	—	—	—
— *Present analysis*					
LW4	0·0931	0·4443	0·7498	3·1726	3·2465
— σ_{zz} included					
D3i	0·0932	0·4443	0·7498	3·1737	3·2485
D2i	0·0934	0·4443	0·7498	3·4924	3·5699
D1i	0·1029	0·4443	0·7502	3·4924	3·5883
— σ_{zz} discarded					
D3d	0·1024	0·4443	0·8311	3·1737	3·2735
D2d	0·1029	0·4443	0·8311	3·4925	3·5895
D1d	0·1029	0·4443	0·8312	3·4250	3·5880
			$mh/a = 0{\cdot}2$, $nh/a = 0{\cdot}2$		
Exact	0·3421	0·8886	1·4923	3·2648	3·5298
LWM-1	0·3416	0·8886	1·4932	3·2656	3·5398
R&P	0·3411	—	—	—	—
— *Present analysis*					
LW4	0·3421	0·8886	1·4923	3·2656	3·5309
— σ_{zz} included					
D3i	0·3421	0·8886	1·4923	3·2657	3·5355
D2i	0·3456	0·8886	1·4925	3·4555	3·5763
D1i	0·3763	0·8886	1·4959	3·5763	3·7627
— σ_{zz} discarded					
D3d	0·3701	0·8886	1·6623	3·2656	3·6255
D2d	0·3763	0·8886	1·6623	3·5763	3·9257
D1d	0·3763	0·8886	1·6623	3·5763	3·7627

agreement between present mixed analysis and exact solution has to be registered. Better results with respect to standard classical displacement formulation are found. The value quoted in brackets accompanying some of the numerical results in Table 7 indicates the circumferential wave number, *n*, for which the fundamental frequency was detected. All the theories considered in reference [50] neglect transverse normal stress effects. Uniform UNI, parabolic PAR and hyperbolic HYP transverse shear stress distribution in the thickness shell direction where

TABLE 6

Comparison of present mixed analysis to exact [6] *and to other refined models on the lowest* 10 *circular frequency parameters* $\omega h\sqrt{\rho/E_T}$ *Simply supported square plates* $a/h = 10$. *Cross-ply skew-symmetric laminates* 0/90/0/90 $E_L = 25{\cdot}1 \times 10^6$ *psi*, $E_T = 4{\cdot}8 \times 10^6$ *psi*, $E_z = 0{\cdot}75 \times 10^6$ *psi*, $G_{LT} = 1{\cdot}36 \times 10^6$ *psi*, $G_{Lz} = 1{\cdot}2 \times 10^6$ *psi*, $G_{Tz} = 0.47 \times 10^6$ *psi*, $\nu_{LT} = 0{\cdot}036$, $\nu_{Lz} = 0{\cdot}25$, $\nu_{TT} = 0{\cdot}171$

Nosier *et al.* 1993					Present		
Exact	LWM-2	R&P	LW4	M3i	M3d	D3i	D3d
			$m = n = 1$				
0·06621	0·06622	0·06789	0·06621	0·06627	0·06635	0·06774	0·06781
0·54596	0·54600	0·54845	0·54596	0·54729	0·54733	0·54808	0·54808
0·59996	0·59999	0·60261	0·59996	0·60119	0·60263	0·60197	0·60340
1·2425	1·2435	1·4237	1·2425	1·2436	1·3055	1·2438	1·4201
1·2988	1·2996	1·4535	1·2987	1·3337	1·3357	1·4204	1·4504
1·3265	1·3274	—	1·3265	1·3055	2·6920	1·4482	2·9165
2·3631	2·3698	—	2·3631	2·6914	2·7018	2·9145	2·9253
2·3789	2·3856	—	2·3789	2·7066	4·9080	2·9305	5·6706
2·4911	2·4983	—	2·4911	2·8356	4·9095	3·0745	5·6757
3·6661	3·6939	—	2·6662	4·9061	5·9554	5·1758	—
			$m = 2, n = 1$				
0·15194	0·15198	0·16065	0·15194	0·15224	0·15231	0·15947	0·15953
0·63875	0·63879	0·64119	0·63875	0·63999	0·64052	0·64072	0·64122
1·0761	1·0765	1·09931	1·0761	1·0869	1·0902	1·0924	1·0958
1·2417	1·2426	1·4651	1·2417	1·2434	1·3499	1·2439	1·4616
1·3425	1·3433	1·7525	1·3425	1·3492	1·6566	1·4611	1·7327
1·6323	1·6336	—	1·6323	1·6536	2·7117	1·7295	2·9347
2·3869	2·3936	—	2·3869	2·7128	2·8525	2·9349	3·0713
2·4844	2·4917	—	2·4844	2·8281	4·9172	3·0582	5·6802
2·5614	2·5678	—	2·5614	2·8690	4·9848	3·1056	5·7638
3·6778	3·7051	—	3·6778	4·9171	5·9663	5·1807	—

considered as well as the two cases of interlaminar discontinuous $_{ds}$ and continuous $_{cs}$ shear stresses (see reference [50] for further details). Uniform distribution cases do not fulfill static conditions at the top and bottom shell surfaces. *ZZL* results refer to analysis in reference [66] which is the same as that of UNI_{cs}. The fundamental mode, e.g. n-values can be erroneously predicted by simplified analysis. The importance of fulfilling the interlaminar transverse shear stress continuity has been confirmed by the present analysis. Nevertheless, the role played by the transverse normal stress should be underlined. Such a role could become more predominant for thicker shells. Comments made in the above discussion of Table 6 results have been confirmed by Table 7.

A few further parametric studies have been presented to provide some insight into the effects of variation in material and geometric characteristics of laminated shells on their vibration characteristic. Tables 8 and 9 consider laminated circular cylinders having both symmetric and skew-symmetric lamination with respect to

TABLE 7

Effect of radii to length ratio R/a on $\omega \times a^2\sqrt{\rho/h^2E_T}$. Comparison to exact solution by Ye and Soldatos [14] and to other refined analyses. $a/h = 10$, $m = 1$, $n = 2$ unless given in brackets. Three-layered ringed shell 0/90/0, $h_1 = h_3 = h_2/2$. $E_L/E_T = 25$, $G_{LT}/E_T = 0{\cdot}5$, $G_{TT}/E_T = 0{\cdot}2$, $\nu_{LT} = \nu_{TT} = 0{\cdot}25$

R_β/a	5	10	50	100
Exact	$10{\cdot}305^{14}$	$10{\cdot}027^{22}$	$9{\cdot}834^{24}$	9·815
PAR$_{ds}$	10·496	10·223	$10{\cdot}032^{26}$	10·013
HYP$_{ds}$	10·496	10·226	$10{\cdot}036^{26}$	10·018
UNI$_{cs}$	10·462	10·187	$9{\cdot}996^{28}$	9·977
PAR$_{cs}$	10·329	10·051	$9{\cdot}859^{26}$	9·840
HYP$_{cs}$	10·328	10·050	$9{\cdot}858^{26}$	9·839
ZZL	$10{\cdot}462^{14}$	$10{\cdot}187^{24}$	$9{\cdot}996^{16}$	$9{\cdot}971^{4}$
— *Present analysis*				
LW4	$10{\cdot}305^{14}$	$10{\cdot}027^{22}$	$9{\cdot}834^{26}$	9·815
M3i	$10{\cdot}309^{14}$	$10{\cdot}030^{22}$	$9{\cdot}837^{26}$	9·818
M3d	$10{\cdot}324^{14}$	$10{\cdot}043^{22}$	$9{\cdot}847^{26}$	9·828
M1i	$10{\cdot}328^{14}$	$10{\cdot}046^{22}$	$9{\cdot}850^{26}$	9·831
M1d	$10{\cdot}328^{14}$	$10{\cdot}046^{22}$	$9{\cdot}850^{26}$	9·831
D3i	$10{\cdot}453^{14}$	$10{\cdot}179^{22}$	$9{\cdot}988^{26}$	9·969
D3d	$10{\cdot}470^{14}$	$10{\cdot}193^{22}$	$9{\cdot}998^{26}$	9·979
D1i	$11{\cdot}318^{14}$	$11{\cdot}063^{20}$	$10{\cdot}879^{20}$	10·862
D1d	$11{\cdot}318^{14}$	$11{\cdot}064^{20}$	$10{\cdot}880^{20}$	10·862

the middle surface for which approximate three dimensional solution were given by Noor and Rarig [11]. The fibers of the different layers alternate between the longitudinal α and circumferential β directions, with the fibers of the top layer running in the circumferential direction. The total thickness of the circumferential and longitudinal layers in each shell was the same. The material characteristics of the individual layers were taken to be those of typical of high-modulus fibrous composites, namely $G_{LT}/E_T = G_{Lz}/E_T = 0{\cdot}6$, $G_{TT}/E_T = 0{\cdot}5$, $\nu_{LT} = \nu_{TT} = 0{\cdot}25$. The degree of orthotropy of the individual layers E_L/E_T, the thickness ratio R_β/h as well as circumferential modes n were varied in the investigations. Accurate description of very thick shells with increasing number of layers demand a layer-wise description. Note that D3i results are in some case more accurate than those related M3d analyses. In such a case σ_{zz} plays a predominant role with respect to zigzag effects and interlaminar equilibria. It is concluded that the approximation introduced by discarding σ_{zz} are very much influenced by geometrical and mechanical parameters as well as by laminate stacking sequence.

The problems investigated previously have been restricted to a laminated structure with almost constant transverse mechanical properties in the thickness direction (the Young's modulus is constant in the z-shell direction and the variation of $\tilde{C}_{13}$ and $\tilde{C}_{23}$ in the same direction is at least one order of magnitude less than the other layer constant). Previous plate analyses [58] showed that the zigzag form of

TABLE 8

Effect of degree of orthotropy of the individual layers E_L/E_T on $\omega \times 10\sqrt{\rho h^2/E_T}$. Comparison to 3D solutions by Noor and Rarig [11]. $h/R_\beta = 0{\cdot}2$, $a/R_\beta = 1, m = 1, n = 4$

	N_l	E_L/E_T 3	10	40
3D	2	2·3141	2·5464	2·9262
LW4		2·3141	2·5464	2·9263
M3i		2·3152	2·5619	2·9791
M3d		2·3721	2·5966	2·9999
D3i		2·3153	2·5640	3·0049
D3d		2·3722	2·5986	3·0247
3D	3	2·3173	2·6542	3·1675
LW4		2·3173	2·6542	3·1998
M3i		2·3226	2·6659	3·1998
M3d		2·3718	2·6943	3·2221
D3i		2·3227	2·6668	3·2096
D3d		2·3719	2·6953	3·2316
3D	5	2·3767	2·8245	3·4631
LW4		2·3767	2·8245	3·4633
M3i		2·3807	2·8336	3·4887
M3d		2·4268	2·8555	3·5038
D3i		2·3816	2·8371	3·5011
D3d		2·4278	2·8591	3·5163
3D	10	2·4357	2·9856	3·7506
LW4		2·4357	2·9856	3·7507
M3i		2·4397	2·9945	3·7692
M3d		2·4849	3·0133	3·7784
D3i		2·4404	2·9967	3·7763
D3d		2·4857	3·0155	3·7855

u_z had in fact barely been exhibited by the exact analysis. In order to investigate transverse stress effects for highly transverse anisotropic structures a multilayered plate and spherical panel with non-constant distribution of Young modulus E_z in the thickness direction has been considered in Figure 4 and Table 10. Three layered thick and thin flat and spherical panels constituted by isotropic ($\nu = 0{\cdot}3$) layers has been investigated. The panels are unsymmetrically laminated with $E^1/E^2 = 10$; $E^3/E^2 = 100$ where E^k ($k = 1, 2, 3$) are the Young's moduli of the three layers. The same ratios have been used for mass density. E^2 and ρ^2 have been used in the quoted non-dimensioned amplitudes. Figure 4 shows an evident zigzag behaviour for the transverse displacement in the thickness spherical shell directions. Table 10 shows that the interlaminar equilibria and zigzag effect are more significant with respect to the previously cited results. D3i analyses are never more accurate than M3d analyses.

TABLE 9

Effect of thickness to radii ratio $h/R\beta$ on $\omega \times 10\sqrt{\rho h^2/E_T}$. Comparison to 3D solutions by Noor and Rarig [11]. $E_L/E_T = 30$, $a/R_\beta = 1$, $m = 1$

	h/R_β	n = 2	4	6
		$N_l = 2$		
3D	0·05	0·8165	0·5385	0·4218
LW4		0·8165	0·5385	0·4218
M3i		0·8163	0·5391	0·4227
M3d		0·8177	0·5404	0·4245
D3i		0·8164	0·5391	0·4228
D3d		0·8177	0·5404	0·4246
3D	0·40	7·5953	6·9568	7·9209
LW4		7·5972	6·9575	7·9205
M3i		7·7327	7·1734	8·1133
M3d		7·7569	7·2205	8·1908
D3i		7·8030	7·2619	8·2181
D3d		7·8208	7·3046	8·2919
		$N_l = 10$		
3D	0·05	0·8410	0·5832	0·5027
LW4		0·8410	0·5832	0·5027
M3i		0·8410	0·5834	0·5029
M3d		0·8415	0·5842	0·5045
D3i		0·8410	0·5834	0·5030
D3d		0·8415	0·5842	0·5046
3D	0·40	8·6111	8·4732	9·8040
LW4		8·6117	8·4736	9·8043
M3i		8·6765	8·5730	9·9352
M3d		8·6778	8·5939	9·9822
D3i		8·6896	8·5957	9·9643
D3d		8·6907	8·6158	10·0103

TABLE 10

Effect of thickness ratio a/h on $\omega \times 1.\ E4\sqrt{\rho^2 h^2/E_T^2}$. Three layered, squared flat and spherical panels ($R_\alpha/a = 2{\cdot}5$) made of isotropic layers ($\nu = 0{\cdot}3$). $m = n = 1$

a/h	4	10	100
Flat panels			
LW4	1695·0	385·4	4·634
M3i	1717·0	386·4	4·634
M3d	1825·0	395·3	4·635
D3i	2421·0	448·9	4·644
D3d	2658·0	455·5	4·645
Spherical panels			
LW4	1954·0	560·9	41·69
M3i	2007·0	566·2	41·70
M3d	2113·0	578·9	41·72
D3i	2501·0	612·5	41·70
D3d	2904·0	627·9	41·72

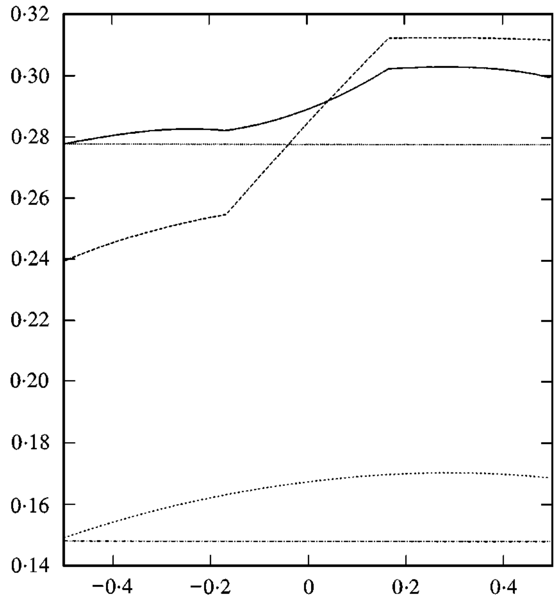

Figure 4. $U_z \times 100E_T h^3/(p_{z_t}^{N_l} a^4)$ versus z. Three-layered spherical panel made of isotropic layers, $a/h = 4$. LW4—; M3i ----; D3i ····; M3d ----; D3d -·-·-·-·.

6. CONCLUDING REMARKS

The mixed theory originally proposed by Toledano and Murakami has been reformulated and extended to dynamic analyses of plates and double-curved shells. Transverse normal stress effects have been compared and evaluated by allowing different polynomial orders in the displacement expansions. Classical theories have been considered for comparison purpose. From the investigation carried out the following main remarks can be made.

1. The *a priori* fulfillment of the interlaminar continuity for σ_{zz} makes mixed models more attractive than other available models which violate such a continuity.
2. Koiter's recommendation [1] concerning isotropic shells: *a refinement of Love's first approximation theory is indeed meaningless, in general, unless the effects of transverse shear and normal stresses are taken into account at the same time*, could be re-written for the case of multilayered shells as: *a refinement of … … unless the effects of interlaminar continuous transverse shear and normal stresses are taken into account at the same time.*
3. In any case a very accurate description of the vibrational response of highly anisotropic, thick and very thick z-shells requires layer-wise description.

REFERENCES

1. W. T. Koiter 1959 *Proceedings of Symposium on the Theory of Thin Elastic Shells, August* 1959, *North-Holland, Amsterdam*, 12–23. A consistent first approximations in the general theory of thin elastic shells.

2. A. N. Goldenvaizer 1961 *Theory of Thin Elastic Shells. International Series of Monograph in Aeronautics and Astronautics*. New York: Pergamon Press.
3. P. Cicala 1965 *Systematic Approach to Linear Shell Theory*. Torino: Levrotto & Bella.
4. R. D. Mindlin, A. Schacknow and H. Deresiewicz 1956 *Journal of Sound and Vibration* **12**, 187–195. An exact analysis for vibration of simply supported homogeneous and laminated thick rectangular plates.
5. N. J. Pagano 1969 *Journal of Composite Materials* **3**, 398–411. Exact solutions for composite laminates in cylindrical bending.
6. S. Srinivas, C. V. Joga Rao and A. K. Rao 1970 *Journal of Applied Mechanics* **23**, 430–436. Flexural vibration of rectangular plates.
7. A. K. Noor 1973 *American Institute of Aeronautics and Astronautics Journal* **11**, 1038–1039. Free vibration of multilayered plates.
8. A. K. Noor and W. S. Burton 1989 *Composite Structures* **11**, 183–204. Stress and free vibration analyses of multilayered composite plates.
9. J. G. Ren 1987 *Composite Science and Techonology* **29**, 169–187. Exact solutions for laminated cylindrical shells in cylindrical bending.
10. T. K. Varadan and K. Bhaskar 1991 *Composite Structures* **17**, 141–156. Bending of laminated orthotropic cylindrical shells — an elasticity approach.
11. A. K. Noor and P. L. Rarig 1974 *Computer Methods in Applied Mechanics and Engineering* **3**, 319–334. Three-dimensional solutions of laminated cylinders.
12. A. K. Noor and W. S. Peters 1989 *Journal of Structural Engineering, ASCE*, **115**, 69–89. Stress, vibration and buckling of multilayered cylinders.
13. A. K. Noor and W. S. Peters 1989 *Journal of Engineering Mechanics, ASCE*, **115**, 1225–1245. A posteriori estimates for shear correction factors in multilayered composite cylinders.
14. J. Q. Ye and K. P. Soldatos 1994 *Composite Engineering* **4**, 429–444. Three-dimensional vibration of laminated cylinders and cylindrical panels with symmetric or antisymmetric cross-ply lay-up.
15. O. A. Fettahlioglu and C. R. Steele 1974 *Journal of Applied Mechanics* 753–758. Asymptotic solutions for orthotropic non-homogeneous shells of revolution.
16. C. Wu, J. Tarn and S. Tang 1997 *Journal of Sound and Vibration* **35**, 1953–79. A refined asymptotic theory for dynamic analysis of doubly curved laminated shells.
17. V. L. Berdichevsky 1979 *PMM* **43**, 664–667. Variational-asymptotic method of shell theory construction.
18. G. E. O. Widera and D. L. Logan 1980 *Journal of Engineering Mechanics Division, ASCE* **106**, 1053–1073. A refined theories for non-homogeneous anisotropic, cylindrical shells: Part I-derivation.
19. G. E. O. Widera and H. Fan 1988 *Journal of Applied Mechanics* **110**, 102–105. On the derivation of a refined theory for non-homogeneous anisotropic shells of revolution.
20. V. L. Berdichevsky and V. Misyura 1992 *Journal of Applied Mechanics* **59**, S217–S223. Effect of accuracy loss in classical shell theory.
21. D. H. Hodges, B. W. Lee and A. R. Atilgan 1993 *American Institute of Aeronautics and Astronautics Journal* **31**, 1674–1983. Application of the variational-asymptotic method to laminated composite plates.
22. V. G. Sutyrin and D. H. Hodges 1996 *International Journal of Solids and Structures* **33**, 3649–3671. On asymptotically correct linear laminated plate theory.
23. V. G. Sutyrin 1997 *Journal of Applied Mechanics*, **64**, 905–915. Derivation of plate theory accounting asymptotically correct shear deformation.
24. E. I. Grigolyuk and G. M. Kulikov 1988 *Mekhanica Kompozitnykh Materialov* No. 2, 287–298. General direction of the development of the theory of shells.
25. R. K. Kapania and S. Raciti 1989 *American Institute of Aeronautics and Astronautics Journal* **27**, 923–946. Recent advances in analysis of laminated beams and plates.
26. R. K. Kapania 1989 *Journal of Pressure Vessel Technology* **111**, 88–96. A review on the analysis of laminated shells.

27. A. K. NOOR and W. S. BURTON 1989 *Applied Mechanics Review* **41**, 1–18. Assessment of shear deformation theories for multilayered composite plates.
28. A. K. NOOR and W. S. BURTON 1990 *Applied Mechanics Review* **43**, 67–97. Assessment of computational models for multilayered composite shells.
29. A. K. NOOR, S. BURTON and C. W. BERT 1996 *Applied Mechanics Review* **49**, 155–199. Computational model for sandwich panels and shells.
30. K. P. SOLDATOS and T. TIMARCI 1993 *Composite Structures* **25**, 165–171. A unified formulation of laminated composites, shear deformable, five-degrees-of-freedom cylindrical shell theories.
31. J. N. REDDY 1997 *Mechanics of Laminated Composite Plates, Theory and Analysis*. Boca Raton: CRC Press.
32. T. HSU and J. T. WANG 1970 *American Institute of Aeronautics and Astronautics Journal* **8**, 2141–2146. A theory of laminated cylindrical shells consisting of layers of orthotropic laminae.
33. Y. K. CHEUNG and C. I. WU 1972 *Journal of Sound and Vibration* **24**, 189–200. Free vibrations of thick, layered cylinders having finite length with various boundary conditions.
34. S. SRINIVAS 1973 *Journal of Sound and Vibration* **30**, 495–50. A refined analysis of composite laminates.
35. C. T. SUN and J. M. WHITNEY 1973 *American Institute of Aeronautics and Astronautics Journal* **11**, 372–398. On the theories for the dynamic response of laminated plates.
36. E. J. BARBERO, J. N. REDDY and J. L. TEPLY 1990 *American Institute of Aeronautics and Astronautics Journal* **28**, 544–553. General two-dimensional theory of laminated cylindrical shells.
37. K. N. CHO, C. W. BERT and A. G. STRIZ 1991 *Journal of Sound and Vibration* **145**, 429–442. Free vibrations of laminated rectangular plates analyzed by higher order individual-layer theory.
38. A. NOSIER, R. K. KAPANIA and J. N. REDDY 1993 *American Institute of Aeronautics and Astronautics Journal* **31**, 2335–2346. Free vibration analysis of laminated plates using a layer-wise theory.
39. P. GAUDENZI, R. BARBONI and A. MANNINI 1995 *Composite Structures*, **30**, 427–440. A finite element evaluation of single-layer and multi-layer theories for the analysis of laminated plates.
40. E. CARRERA 1998 *American Institute of Aeronautics and Astronautics Journal* **36**, 830–839. Evaluation of layer-wise mixed theories for laminated plates analysis.
41. E. CARRERA 1998 *Journal of Applied Mechanics* **65**, 820–828. Layer-wise mixed models for accurate vibration analysis of multilayered plates.
42. E. CARRERA 1998 *Journal of Applied Mechanics*. A Reissner's mixed variational theorem applied to vibrational analysis of multilayered shell. vol 66 63–78.
43. F. B. HILDEBRAND, E. REISSNER and G. B. THOMAS 1940 *NACA TN-1833*, Washington, D.C. Notes on the foundations of the theory of small displacement of orthotropic shells.
44. K. H. LO R. M. CHRISTENSEN and E. M. WU 1977 *Journal of Applied Mechanics* **44**, 669–676. A higher-order theory of plate deformation, Part 2: laminated plates.
45. S. A. AMBARTSUMIAN 1968 *PMM* **22**, 226–237. On general theory of anisotropic shells.
46. J. M. WHITNEY 1969 *Journal of Composite Materials* **3**, 534–547. The effects of transverse shear deformation on the bending of laminated plates.
47. B. K. RATH and Y. C. DAS 1973 *Journal of Sound and Vibration* **28**, 737–757. Vibration of layered shells.
48. J. G. REN 1986 *Composite Science and Techonology* **26**, 225–239. A new theory for laminated plates.
49. M. CHO and R. R. PARMERTER 1993 *American Institute of Aeronautics and Astronautics Journal* **31**, 1299–1305. Efficient higher order composite plate theory for general lamination configurations.

50. T. Timarci and K. P. Soldatos 1995 *Journal of Sound and Vibration* **187**, 609–624. Comparative dynamic studies for symmetric cross-ply circular cylindrical shells on the basis a unified shear deformable shell theories.
51. A. Idlbi, M. Karama and M. Touratier 1997 *Composite Structures*, **37**, 173–184. Comparison of various laminated plate theories.
52. A. Toledano and H. Murakami 1987 *International Journal of Solids and Structures* **23**, 111–131. A higher-order laminated plate theory with improved in-plane responses.
53. E. Reissner 1984 *International Journal for Numerical Methods in Engineering* **20**, 1366–1368. On a certain mixed variational theory and a proposed applications.
54. E. Carrera 1995 *Atti Accademia delle Scienze di Torino, Memorie Scienze Fisiche* **19–20**, 49–87. A class of two dimensional theories for multilayered plates analysis.
55. K. Bhaskar and T. K. Varadan 1992 *Journal of Pressure Vessel Technology* **114**, 115–119. Reissner's new mixed variational principle applied to laminated cylindrical shells.
56. H. Jing and K. Tzeng 1993 *American Institute of Aeronautics and Astronautics Journal* **31**, 765–773. Refined shear deformation theory of laminated shells.
57. E. Carrera 1991 *Journal of Sound and Vibration* **151**, 405–433. The effects of shear deformation and curvature on buckling and vibrations of cross-ply laminated composite shells.
58. E. Carrera Journal of Applied Mechanics, Transverse Normal Stress Effects in Multilayered Plates [in press].
59. H. Kraus 1967 *Thin Elastic Shells*, New York: Wiley.
60. L. Librescu 1975 *Elasto-statics and Kinetics of Anisotropic and Heterogeneous Shell-Type Structures*. Leyden, Netherland: Noordhoff Int.
61. H. Murakami 1986 *Journal of Applied Mechanics* **53**, 661–666. Laminated composite plate theory with improved in-plane response.
62. S. T. Dennis and A. N. Palazotto 1991 *American Institute of Aeronautics and Astronautics Journal* **29**, 647–650. Laminated shell in cylindrical bending, two-dimensional approach vs exact.
63. M. Di Sciuva 1993 *Composite Structures* **47**, 91–105. A general quadrilater multilayered plate element with continuous interlaminar stresses.
64. J. N. Reddy and C. F. Liu 1985 *International Journal of Engineering Science* **23**, 319–330. A higher-order shear deformation theory of laminated elastic shells.
65. J. N. Reddy and N. D. Phan 1985 *Journal of Sound and Vibration* **98**, 157–170. Stability and vibration of isotropic, orthotropic, and laminated plates according to a higher order shear deformation theory.
66. M. Di Sciuva and E. Carrera 1992 *Journal of Applied Mechanics* **59**, 222–223. Elasto-dynamic behavior of relatively thick, symmetrically laminated, anisotropic circular cylindrical shells.